[26] W. B. Kleijn and K. Paliwal, *Speech Coding and Synthesis*. Amsterdam, The Netherlands: Elsevier, 1995.
[27] F. Itakura, "Line spectrum representation of linear predictor coefficients of speech signals," *J. Acoust. Soc. Amer.*, vol. 57, no. S35(A), 1975.
[28] K. K. Paliwal and B. S. Atal, "Efficient vector quantization of LPC parameters at 24 bits/frame," *IEEE Trans. Speech Audio Process.*, vol. 1, no. 1, pp. 3–14, Jan. 1993.
[29] S. Bruhn, P. Blocher, K. Hellwig, and J. Sjoberg, "Concepts and solutions for link adaptation and inband signalling for the GSM AMR speech coding standard," in *Proc. Vehicular Technology Conf.*, Houston, TX, May 1999.
[30] R. A. Salami, C. Laflamme, J. P. Adoul, and D. Massaloux, "A toll quality 8 kb/s speech codec for the personal communications system (PCS)," *IEEE Trans. Veh. Technol.*, vol. 43, no. 4, pp. 808–816, Aug. 1994.
[31] "Coding of Speech at 8 kbit/s Using Conjugate-Structure Algebraic Code-Excited Linear Prediction (CS-ACELP)," ITU Recommendation G.729, International Telecommunication Union, Geneva, Switzerland, 1995.
[32] R. Steele and L. Hanzo, *Mobile Radio Communications*, 2nd ed. Piscataway, NJ: IEEE Press, 1999.
[33] J. H. Chen and A. Gersho, "Adaptive postfiltering for quality enhancement of coded speech," *IEEE Trans. Speech Audio Process.*, vol. 3, no. 1, pp. 59–71, Jan. 1995.
[34] *GSM 05.09: Digital Cellular Telecommunications System (Phase 2+); Link Adaptation.*, ver. 7.0.0, Release, 1998.
[35] N. S. Szabo and R. I. Tanaka, *Residue Arithmetic and Its Applications to Computer Technology*. New York: McGraw-Hill, 1967.
[36] F. J. Taylor, "Residue arithmetic: A tutorial with examples," *IEEE Computer*, vol. 17, no. 5, pp. 50–62, May 1984.
[37] H. Krishna, K. Y. Lin, and J. D. Sun, "A coding theory approach to error control in redundant residue number systems—Part I: Theory and single error correction," *IEEE Trans. Circuits Syst. II, Analog Digit. Signal Process.*, vol. 39, no. 1, pp. 8–17, Jan. 1992.
[38] J. D. Sun and H. Krishna, "A coding theory approach to error control in redundant residue number systems—Part II: Multiple error detection and correction," *IEEE Trans. Circuits Syst. II, Analog Digit. Signal Process.*, vol. 39, no. 1, pp. 18–34, Jan. 1992.
[39] L.-L. Yang and L. Hanzo, "Performance of residue number system based DS-CDMA over multipath channels using orthogonal sequences," *Eur. Trans. Commun.*, vol. 9, no. 6, pp. 525–535, Nov./Dec. 1998.
[40] L.-L. Yang and L. Hanzo, "Residue number system arithmetic based orthogonal signalling schemes for AWGN and Rayleigh channels," *IEEE Trans. Veh. Technol.* vol. 51, no. 6, pp. 1534–1546, Nov. 2002.
[41] L.-L. Yang and L. Hanzo, "Residue number system arithmetic based orthogonal signalling schemes for AWGN and Rayleigh channels," *IEEE Trans Veh. Technol.* vol. 51, no. 6, pp. 1547–1559, Nov. 2002.
[42] A. Klein, G. K. Kaleh, and P. W. Baier, "Zero forcing and minimum mean square error equalization for multiuser detection in code division multiple access channels," *IEEE Trans. Veh. Technol.*, vol. 45, no. 3, pp. 276–287, May 1996.
[43] C. Tang, "An intelligent learning scheme for adaptive modulation," in *Proc. IEEE Vehicular Technology Conf.*, Atlantic City, NJ, Oct. 2001, pp. 144–148.
[44] J. M. Torrance and L. Hanzo, "On the upper bound performance of adaptive QAM in slow Rayleigh fading channel," *Electron. Lett.*, pp. 169–171, Apr. 1996.
[45] M. Failli, "Digital Land Mobile Radio Communications COST 207," European Commission, Luxembourg, Tech. Rep., 1989.

Multiuser Detection Assisted Time- and Frequency-Domain Spread Multicarrier Code-Division Multiple-Access

Lie-Liang Yang, Wei Hua, and Lajos Hanzo

***Abstract*—In this contribution, we study a reduced-complexity multiuser detection aided multicarrier direct-sequence code-division multiple-access (MC DS-CDMA) scheme, which employs both time (T)-domain and frequency (F)-domain spreading. We investigate the achievable detection performance in the context of synchronous TF-domain spread MC DS-CDMA when communicating over an additive white Gaussian noise (AWGN) channel. Five detection schemes are investigated, which include the single-user correlation based detector, the joint TF-domain decorrelating multiuser detector (MUD), the joint TF-domain MMSE MUD, the separate TF-domain decorrelating/MMSE MUD, and the separate TF-domain MMSE/decorrelating MUD. Our simulation results show that the separate TF-domain MUD schemes are capable of achieving a similar bit error rate (BER) performance to that of the significantly more complex joint TF-domain MUD schemes.**

***Index Terms*—Code-division multiple-access (CDMA), decorrelating, frequency-domain spreading, joint detection, minimum mean square error (MMSE), multicarrier (MC), multiuser detection, separate detection, time-domain spreading.**

I. Introduction

In the context of direct-sequence (DS) code-division multiple-access (DS-CDMA) communications, there are two types of spread-spectrum schemes. The first of these spread-spectrum schemes [1]–[3] spreads the original data stream using a signature code in the time (T)-domain, and the spread-spectrum signal is transmitted using a single-carrier. In contrast, the second DS spread-spectrum scheme [4]–[7] spreads the original data stream to a number of subcarriers using a signature code in the frequency (F)-domain, and each chip of the resultant spread-spectrum signal is transmitted by a different carrier. Hence, this scheme is also referred to as multicarrier CDMA (MC-CDMA) in the literature [5], [6], [8], [9]. Furthermore, there is a family of multicarrier CDMA in which each subcarrier signal constitutes a T-domain DS spread signal, but no F-domain spreading is employed. This family of multicarrier CDMA is usually referred to as MC DS-CDMA [5], [10]–[16]. An amalgam of these spread-spectrum schemes was proposed in [17]. This extended spread-spectrum scheme spreads the transmitted data stream using two signature codes, where one of the signature codes corresponds to the T-domain spreading, while the other corresponds to the F-domain spreading. Since the proposed multicarrier DS-CDMA scheme employs both the previously mentioned T-domain spreading and F-domain spreading, it is referred to as TF-domain spread MC DS-CDMA.

The benefits of employing both T-domain spreading and F-domain spreading in MC DS-CDMA systems are multifold. First, the future generations of broadband multiple-access systems [18] are expected to have a bandwidth on the order of tens or even hundreds of MHz. When single-carrier based DS-CDMA or MC-CDMA using solely T-domain spreading or solely F-domain spreading is utilized, the total system bandwidth is related to either the T-domain spreading factor or to the

Manuscript received June 18, 2004; revised April 18, 2005. This work was supported by the Virtual Centre of Excellence in Mobile and Personal Communications, Mobile VCE, and EPSRC. The review of this paper was coordinated by Prof. T. Lok.

The authors are with the Department of Electronics and Computer Science, University of Southampton, Southampton, SO17 1BJ U.K. (e-mail: lh@ecs.soton.ac.u.k).

Digital Object Identifier 10.1109/TVT.2005.861177

F-domain spreading factor. Consequently, these broadband systems may inevitably require a high chip-rate and long spreading codes. In the proposed TF-domain spread MC DS-C MA scheme, the total system bandwidth is related to the product of the T-domain spreading factor and the F-domain spreading factor, as we will see in our forthcoming discourse. Therefore, a relatively low-chip-rate and short spreading codes can be employed in TF-domain spread MC DS-CDMA schemes. Second, the broadband multiple-access systems are expected to support a wide range of services and bit rates, as well as a number of simultaneous users. It is widely recognized that in CDMA-based communications, multiuser detection [19] is capable of suppressing the multiuser interference and of significantly increasing the system's user capacity. When a single-carrier DS-CDMA or a MC-CDMA, which uses high spreading factors, is invoked for the sake of supporting a large number of users, the employment of advanced multiuser detection algorithms becomes impractical due to their high complexity. By contrast, in the proposed TF-domain spread MC DS-CDMA schemes, simultaneous users can be separated in both the T-domain and the F-domain directions with the aid of unique signature codes. Furthermore, we will show that multiuser detection can be carried out separately in the T-domain and F-domain, while achieving a similar detection performance to that of joint TF-domain processing. Consequently, the detection complexity of the proposed scheme can be significantly decreased compared to that of a conventional single-carrier DS-CDMA or MC-CDMA scheme.

In this contribution, we investigate various detection schemes suitable for demodulating the TF-domain spread MC DS-CDMA signals, and study the detection performance of these detection schemes when communicating over additive white Gaussian noise (AWGN) channels. In addition to the conventional single-user correlator, we also consider two well-known linear multiuser detection algorithms, namely, the decorrelating algorithm [19] and the minimum mean square error (MMSE) algorithm [19]. As we mentioned previously, the TF-domain spread MC DS-CDMA signals can be jointly detected after accomplishing T-domain as well as F-domain despreading. However, detection can also be carried out in two steps, where the first detection step is accomplished in the T-domain, and the second in the F-domain. Therefore, in this contribution, we refer to the former detection scheme as joint TF-domain detection, while to the latter as separate TF-domain detection. Four multiuser detectors (MUD) are considered, which are listed as follows:

1) joint TF-domain decorrelating MUD;
2) joint TF-domain MMSE MUD;
3) separate TF-domain decorrelating/MMSE MUD, where decorrelating is invoked for T-domain detection and MMSE is used for F-domain detection; and
4) separate TF-domain MMSE/decorrelating MUD, where MMSE is used for T-domain detection, and decorrelating is employed for F-domain detection.

The remainder of this contribution is organized as follows: Section II describes the TF-domain spread MC DS-CDMA signal. Section III considers correlation based detection of the TF-domain spread MC DS-CDMA signals. By contrast, in Section IV, we investigate multiuser detections invoked in the context of TF-domain spread MC DS-CDMA system. In Section V, we consider the issue of detection complexity. In Section VI, we provide our simulation results, and in Section VII, we present our conclusions.

II. MC DS-CDMA Signals Using TF-Domain Spreading

The transmitter schematic of MC DS-CDMA using both T-domain and F-domain; i.e., TF-domain spreading, is shown in Fig. 1 in the context of the kth user. At the transmitter side, the binary data stream $b_k(t)$ is first direct-sequence (DS) spread using the T-domain signature sequence $a_k(t)$. Following T-domain DS spreading, the spread signal is divided into M parallel branches, where each branch of the signal is multiplied by the corresponding chip value of the F-domain spreading sequence $c_k = [c_k[1], c_k[2], \ldots, c_k[M]]^T$ of length M. Following F-domain spreading, each of the M branch signals modulates one of the M subcarrier frequencies using binary phase shift keying (BPSK). Then, the M number of subcarrier-modulated substreams are combined for forming the transmitted signal $s_k(t)$. Hence, the transmitted signal of user k can be expressed as

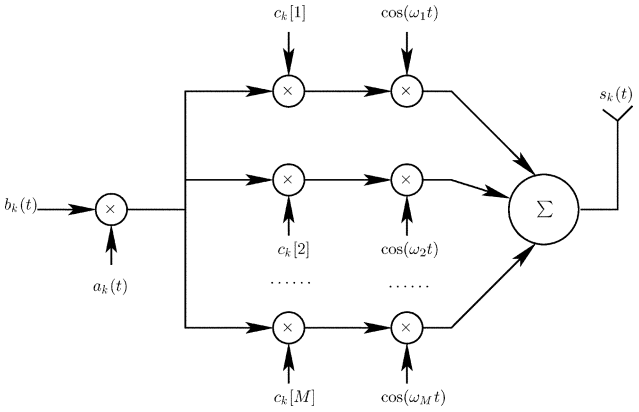

Fig. 1. Transmitter model of MC DS-CDMA using both time-domain and frequency-domain spreading.

$$s_k(t) = \sqrt{\frac{2P}{M}} \sum_{m=1}^{M} b_k(t) a_k(t) c_k[m] \cos(\omega_m t), \quad k = 1, 2, \ldots, K \tag{1}$$

where P represents the identical transmitted power of each user, and $\{\omega_m\}_{m=1}^{M}$ represents the subcarrier frequency set. The binary data stream's waveform $b_k(t) = \sum_{i=0}^{\infty} b_k P_{T_b}(t - iT_b)$ consists of a sequence of mutually independent rectangular pulses of duration T_b, and of amplitude $+1$ or -1, both having an equal probability. In the T-domain spreading sequence $a_k(t) = \sum_{j=0}^{\infty} a_{kj} P_{T_c}(t - jT_c)$ of the kth user, $P_{T_c}(t)$ represents the rectangular T-domain chip waveform, which is defined over the interval $[0, T_c)$. We assume that the T-domain spreading factor is $N = T_b/T_c$, which represents the number of chips per bit-duration, and short T-domain spreading sequences are used. Furthermore, we assume that the subcarrier signals are orthogonal, and that the spectral main-lobes of the subcarrier signals are not overlapping with each other.

In the system studied, K synchronous TF-domain spread MC DS-CDMA signals obeying the form of (1) are transmitted over AWGN channels. We assume that the power received from each user is identical, implying perfect power control. Consequently, the received signal can be expressed as

$$r(t) = \sum_{k=1}^{K} \sqrt{\frac{2P}{M}} \sum_{m=1}^{M} b_k(t) a_k(t) c_k[m] \cos(\omega_m t) + n(t) \tag{2}$$

where $n(t)$ represents the AWGN having zero mean and double-sided power spectrum density of $N_0/2$.

As shown in Fig. 1 and (1), each TF-domain spread MC DS-CDMA signal is spread by two signature sequences, one in the context of the

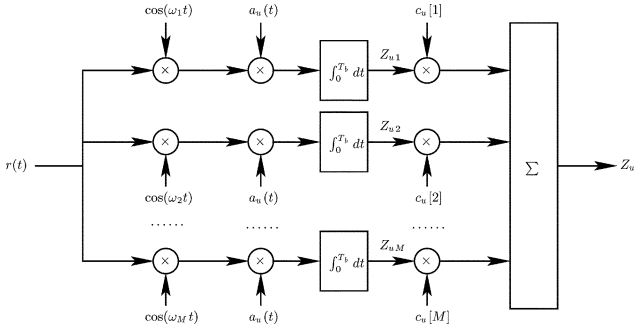

Fig. 2. Receiver model of MC DS-CDMA using both time-domain and frequency-domain spreading.

T-domain, and the other in the F-domain. The employment of concatenated TF-domain spreading is beneficial in the context of various detection schemes, allowing us to achieve a satisfactory tradeoff between the affordable detection complexity and the achievable detection bit error rate (BER) performance. In the following two sections, we analyze the detection of TF-domain spread MC DS-CDMA signals by invoking various detection schemes. Specifically, in Section III, a single-user correlation detector is studied in order to show the similarity of the proposed TF-domain spread MC DS-CDMA and conventional single-carrier DS-CDMA [20] using solely T-domain spreading, as well as that of conventional MC-CDMA [21] using solely F-domain spreading. By contrast, in Section IV, we first investigate two linear multiuser detection schemes, namely the decorrelating MUD and the MMSE MUD in the context of joint TF-domain detection. Then, the combinations of the decorrelating and MMSE MUDs are studied in the context of separate TF-domain detection. Finally, these combined MUDs are compared to the joint TF-domain decorrelating MUD and to the joint TF-domain MMSE based MUD. We now consider the single-user detection of TF-domain spread MC DS-CDMA signals.

III. Single-User Detector

Let the uth user be the user-of-interest, and consider the correlator-based receiver of Fig. 2, which carries out the inverse operations of the functions seen in Fig. 1. As shown in Fig. 2, the output variable related to the first data bit corresponding to the mth subcarrier of the uth user can be expressed as

$$Z_{u\,m} = \int_0^{T_b} r(t) a_u(t) \cos(\omega_m t)\, dt \qquad u = 1, 2, \ldots, K, \quad m = 1, 2, \ldots, M. \tag{3}$$

Upon substituting (2) into (3) and considering the orthogonality between different subcarriers, it can be shown that the output variable $Z_{u\,m}$ of Fig. 2 can be expressed as

$$Z_{u\,m} = \sqrt{\frac{P}{2M}} T_b \left\{ D_{u\,m} + \sum_{\substack{k=1 \\ k \neq u}}^{K} I_{k,m} + N_{u\,m} \right\} \tag{4}$$

where $N_{u\,m}$ is contributed by $n(t)$ of (2), which is a Gaussian random variable having zero mean, and a variance of $MN_0/2E_b$, where $E_b = PT_b$ represents the energy per bit. In (4), $D_{u\,m}$ is the desired output derived by substituting (2) into (3) and setting $k = u$. Hence, $D_{u\,m}$ can be written as $D_m = b_u c_u[m]$. Finally, in (4), $I_{k,m}$ represents the multiuser interference (MUI) imposed by the kth user, which can be expressed as

$$I_{k,m} = \frac{1}{T_b} b_k \int_0^{T_b} a_k(t) a_u(t) c_k[m]\, dt = b_k c_k[m] \times \frac{1}{T_b} \int_0^{T_b} a_k(t) a_u(t)\, dt. \tag{5}$$

In (5), $\rho_{k\,u} = (1)/(T_b) \int_0^{T_b} a_u(t) a_k(t) dt$ represents the correlation factor between the T-domain spreading sequences $a_u(t)$ and $a_k(t)$ of users u and k. Hence, (5) can be rewritten as

$$I_{k,m} = b_k c_k[m] \rho_{u\,k}, \quad k = 1, 2, \ldots, K; \quad m = 1, 2, \ldots, M. \tag{6}$$

Consequently, the output variable corresponding to the first transmitted data bit, the mth subcarrier, and the uth user can be expressed as

$$Z_{u\,m} = \sqrt{\frac{P}{2M}} T_b \left\{ b_u c_u[m] + \sum_{\substack{k=1 \\ k \neq u}}^{K} b_k c_k[m] \rho_{u\,k} + N_{u\,m} \right\} \qquad u = 1, 2, \ldots, K; \quad m = 1, 2, \ldots, M. \tag{7}$$

The decision variable Z_u of Fig. 2, which corresponds to the first transmitted data bit of the reference user u, is obtained by despreading each of the M branch outputs $\{Z_{u\,1}, Z_{u\,2}, \ldots, Z_{u\,M}\}$ using the uth user's F-domain spreading sequence $\mathbf{c}_u$, which can be expressed as

$$\begin{aligned} Z_u &= \sum_{m=1}^{M} c_u[m] Z_{u\,m} \\ &= \sqrt{\frac{P}{2M}} T_b \left\{ \sum_{m=1}^{M} c_u[m] D_{u\,m} + \sum_{\substack{k=1 \\ k \neq u}}^{K} \sum_{m=1}^{M} c_u[m] I_{k,m} + \sum_{m=1}^{M} c_u[m] N_{u\,m} \right\} \\ &= \sqrt{\frac{PM}{2}} T_b \left\{ b_u + \sum_{\substack{k=1 \\ k \neq u}}^{K} b_k \rho_{u\,k} \frac{1}{M} \sum_{m=1}^{M} c_u[m] c_k[m] + N_u \right\} \end{aligned} \tag{8}$$

where $N_u = (1)/(M) \sum_{m=1}^{M} c_u[m] N_{u\,m}$, which is a Gaussian random variable having zero mean and a variance of $N_0/2E_b$. In (8), we define $\beta_{u\,k} = \frac{1}{M} \sum_{m=1}^{M} c_u[m] c_k[m]$, which is the correlation factor between the F-domain spreading sequences $\mathbf{c}_u$ and $\mathbf{c}_k$ assigned to users u and k. Then, (8) can be expressed as

$$Z_u = \sqrt{\frac{PM}{2}} T_b \left\{ b_u + \sum_{\substack{k=1 \\ k \neq u}}^{K} b_k \rho_{u\,k} \beta_{u\,k} + N_u \right\}, \quad u = 1, 2, \ldots, K. \tag{9}$$

Since N_u is a Gaussian distributed random variable, Z_u is also a Gaussian random variable. Its mean is given by $\sqrt{(PM)/(2)} T_b \{b_u + \sum_{\substack{k=1 \\ k \neq u}}^{K} b_k \rho_{u\,k} \beta_{u\,k}\}$, and its variance is given by $MN_0T_b/4$. Finally, with the aid of [19, (3.90)], it can be shown that the BER of the

single-user detector can be expressed as

$$P_b = \frac{1}{2^{K-1}} \sum_{b_1 \in \{-1,+1\}} \cdots \sum_{\substack{b_k \in \{-1,+1\} \\ k \neq u}} \cdots \times \sum_{b_K \in \{-1,+1\}} Q\left(\sqrt{\frac{2E_b}{N_0}}\left[1 - \sum_{\substack{k=1 \\ k \neq u}}^{K} b_k \rho_{uk} \beta_{uk}\right]\right) \quad (10)$$

where $Q(x)$ is the Gaussian Q-function. Furthermore, if the MUI can be approximated by an additive Gaussian variable, then the approximated BER can be expressed as

$$P_b \approx Q\left(\left[\left(\frac{2E_b}{N_0}\right)^{-1} + \sum_{\substack{k=1 \\ k \neq u}}^{K} \rho_{uk}^2 \beta_{uk}^2\right]^{-1/2}\right). \quad (11)$$

Equations (10) and (11) show that for a given signal-to-noise ratio (SNR) per bit value, the BER performance is determined by the MUI, which is a function of both the correlation factors $\{\rho_{uk}\}$ of the T-domain spreading codes, as well as of the correlation factors $\{\beta_{uk}\}$ of the F-domain spreading codes. By contrast, the BER performance of the conventional single-carrier DS-CDMA using T-domain spreading depends solely on the correlation factors of the T-domain spreading codes. Following a similar argument, the BER performance of conventional MC-CDMA using F-domain spreading depends solely on the correlation factors of the F-domain spreading codes. Furthermore, we can see that the BER performance of these CDMA schemes exhibits no substantial difference, provided that the correlation properties of the T- and F-domain spreading schemes are similar, which results in similar MUI values.

IV. Multiuser Detector

In the previous section we have considered single-user detection of the TF-domain spread MC DS-CDMA signals. In this section, we consider the detection of TF-domain spread MC DS-CDMA signals using two well-established MUD algorithms, namely, the decorrelating and the MMSE algorithms, as well as their combinations. Both joint and separate TF-domain detection are investigated. The decision statistics of joint TF-domain detections are obtained after both T-domain and F-domain despreading. By contrast, in the context of separate TF-domain detection, the multiuser TF-domain spread MC DS-CDMA signals are detected in a first step in the T-domain, followed by detection in the F-domain. Since, in this case, the T-domain and F-domain detections are carried out separately, various combinations of MUD algorithms may be invoked for balancing the trade-off between the achievable BER performance and the MUD complexity imposed. In this contribution, for the sake of comparison to joint TF-domain MUDs, we consider the combinations of decorrelating/MMSE and MMSE/decorrelating MUDs, where the first detector in decorrelating/MMSE (or MMSE/decorrelating) is used for T-domain detection, while the second detector in decorrelating/MMSE (or MMSE/decorrelating) is for F-domain detection.

A. Joint TF-Domain Multiuser Detection

By observing (9) and considering the detection of K users, it can be shown that after removing the common factor of $\sqrt{(PM)/(2)}T_b$ associated with all the different users, the decision variables of the K users can be written as

$$\mathbf{Z} = \mathbf{R}\mathbf{b} + \mathbf{n} \quad (12)$$

where we have

$$\mathbf{Z} = [Z_1, Z_2, \ldots, Z_K]^T \quad (13)$$

$$\mathbf{b} = [b_1, b_2, \ldots, b_K]^T \quad (14)$$

$$\mathbf{n} = [N_1, N_2, \ldots, N_K]^T \quad (15)$$

and

$$\mathbf{R} = \begin{pmatrix} 1 & \rho_{12}\beta_{12} & \cdots & \rho_{1K}\beta_{1K} \\ \rho_{21}\beta_{21} & 1 & \cdots & \rho_{2K}\beta_{2K} \\ \vdots & \vdots & \ddots & \vdots \\ \rho_{K1}\beta_{K1} & \rho_{K2}\beta_{K2} & \cdots & 1 \end{pmatrix}. \quad (16)$$

Furthermore, in (12), $\mathbf{n}$ is a zero-mean random Gaussian vector having a covariance of

$$E[\mathbf{n}\mathbf{n}^T] = \frac{N_0}{2E_b}\mathbf{R}. \quad (17)$$

Note that, the product of the T-domain spreading factor of $N = T_b/T_c$ and the F-domain spreading factor of M has a degree of freedom of MN. Therefore, the correlation matrix $\mathbf{R}$ is nonsingular, provided that the number of users K does not exceed MN, i.e., if we have $K \leq MN$. Furthermore, the multiuser detector of the TF-domain spread MC DS-CDMA system is capable of suppressing up to $(MN-1)$ number of interfering users when a T-domain spreading factor of N and an F-domain spreading factor of M are employed.

Based on (12), the K number of TF-domain spread MC DS-CDMA signals can be detected by invoking different MUD algorithms [19]. Let us first consider the joint TF-domain decorrelating detector.

1) Joint TF-Domain Decorrelating Detector: In the context of the decorrelating MUD invoked for the detection of the TF-domain spread MC DS-CDMA signals, the final decision variables associated with $b_k, k = 1, 2, \ldots, K$ are obtained by multiplying both sides of (12) with the inverse of $\mathbf{R}$, i.e., with $\mathbf{R}^{-1}$, which can be expressed as

$$\mathbf{R}^{-1}\mathbf{Z} = \mathbf{b} + \mathbf{R}^{-1}\mathbf{n} \quad (18)$$

and the corresponding data bit b_k is classified according to $\hat{b}_k = \text{sgn}((\mathbf{R}^{-1}\mathbf{Z})_k)$ for $k = 1, 2, \ldots, K$.

According to the analysis of [19, (5.43)], it can be shown that the BER of the joint TF-domain decorrelating MUD can be expressed as

$$P_b = Q\left(\frac{2E_b}{N_0}\sqrt{1 - \mathbf{a}_k^T \mathbf{R}_k^{-1} \mathbf{a}_k}\right) \quad (19)$$

where $\mathbf{a}_k$ is the kth column of the matrix generated by removing the diagonal element of $\mathbf{R}$, and $\mathbf{R}_k$ is the $(K-1) \times (K-1)$ matrix that results by striking out the kth row as well as the kth column of $\mathbf{R}$.

2) Joint TF-Domain MMSE Detector: The MMSE MUD implements the linear mapping, which minimizes the mean-square error between the actual data and the soft outputs of the conventional detector; i.e., $\mathbf{Z}$ of (12). It has been shown in [19] that the MMSE solution is arrived at by multiplying both sides of (12) with the inverse of $(\mathbf{R} + (N_0)/(2E_b)\mathbf{I})$; i.e., with $(\mathbf{R} + (N_0)/(2E_b)\mathbf{I})^{-1}$, which can be expressed as

$$\left(\mathbf{R} + \frac{N_0}{2E_b}\mathbf{I}\right)^{-1}\mathbf{Z} = \left(\mathbf{R} + \frac{N_0}{2E_b}\mathbf{I}\right)^{-1}\mathbf{R}\mathbf{b} + \left(\mathbf{R} + \frac{N_0}{2E_b}\mathbf{I}\right)^{-1}\mathbf{n} \quad (20)$$

while the corresponding data bits b_k are decided according to $\hat{b}_k = \text{sgn}(((\mathbf{R} + (N_0)/(2E_b)\mathbf{I})^{-1}\mathbf{Z})_k)$ for $k = 1, 2, \ldots, K$.

Unfortunately, the analysis of the BER of the joint TF-domain MMSE detector is not as straightforward as that of the decorrelating detector, since the linear MMSE detector does not eliminate the contributions of the interfering users [22].

B. Separate TF-Domain Multiuser Detectors

In the preceding section, the joint detection of the TF-domain spread MC DS-CDMA signals was considered based on the decision statistics obtained after both T-domain and F-domain despreading. The degree of freedom of the joint TF-domain detector is determined by the product of the T-domain spreading factor of N and by the F-domain spreading factor of M. Therefore, joint TF-domain MUDs are capable of suppressing up to $(NM-1)$ number of interferers. According to our analysis in Section IV-A, the joint TF-domain MUDs have to invert a matrix having a rank of K, which may be as high as NM, if the system is fully loaded, i.e., supporting NM users. This statement is valid for both the decorrelating and the MMSE MUDs. We now consider the separate T- and F-domain detection of the TF-domain spread MC DS-CDMA signals, where MUD is carried out first in the T-domain, followed by processing in the F-domain. It can be shown that for the separate TF-domain MUDs, the rank of the matrix invoked for T-domain detection is on the order of N, while that used for F-domain detection is on the order of M.

Note that, generally, in the context of separate TF-domain MUDs, the number of degrees-of-freedom is determined by the sum of the T-domain spreading factor of N and the F-domain spreading factor of M. Therefore, a separate TF-domain MUD is only capable of suppressing up to $(N+M-1)$ number of interfering signals. However, our analysis considering synchronous TF-domain spread MC DS-CDMA shows that separate TF-domain MUDs may also be rendered capable of suppressing up to $(NM-1)$ number of interferers, as will now be discussed.

Let $\{a_1(t), a_2(t), \ldots, a_N(t)\}$ and $\{\mathbf{c}_1, \mathbf{c}_2, \ldots, \mathbf{c}_M\}$ be the N number of T-domain spreading sequences and M number of F-domain spreading sequences, respectively, where $\mathbf{c}_u = [c_u[1] c_u[2] \ldots c_u[M]]^T, u = 1, \ldots, M$ represents an F-domain spreading code. Furthermore, we assume that the number of active users is K, and we introduce a new variable of $\mathcal{K} = \lfloor K/N \rfloor$, where $\lfloor x \rfloor$ represents the smallest integer not less than x. Then, we have $1 \leq \mathcal{K} \leq M$, since $K \leq NM$. With these assumptions, the K number of users supported can be grouped into N user groups, with each group supporting, at most, $\mathcal{K}$ users. Consequently, it can be readily shown that each of the N user groups can be distinguished by assigning one of the N number of T-domain spreading sequences $\{a_1(t), a_2(t), \ldots, a_N(t)\}$. By contrast, the $1 \leq \mathcal{K} \leq M$ number of user signals of a given group are distinguishable with the aid of the $\mathcal{K}$ number of F-domain spreading sequences chosen from the set $\{\mathbf{c}_1, \mathbf{c}_2, \ldots, \mathbf{c}_M\}$. Specifically, for the users belonging to the nth group, the transmitted signals can be expressed as

$$s_n(t) = \sqrt{\frac{2P}{M}} \sum_{\kappa=1}^{\mathcal{K}} \sum_{m=1}^{M} b_{n\kappa}(t) a_n(t) c_\kappa[m] \cos(\omega_m t) \qquad n = 1, 2, \ldots, N \quad (21)$$

where $b_{n\kappa}(t), n = 1, 2, \ldots, N$ is the transmitted waveform of the user corresponding to the nth group $n = 1, 2, \ldots, N$, which is distinguished by the T-domain spreading sequence $a_n(t)$ using the κth F-domain spreading code for $\kappa = 1, 2, \ldots, \mathcal{K}$.

The received signal is the composite multiuser signal constituted by the superposition signals of the N user groups, plus the AWGN contribution of the channel, which can be expressed as

$$r(t) = \sqrt{\frac{2P}{M}} \sum_{n=1}^{N} \sum_{\kappa=1}^{\mathcal{K}} \sum_{m=1}^{M} b_{n\kappa}(t) a_n(t) c_\kappa[m] \cos(\omega_m t) + n(t). \quad (22)$$

The transmitted data of a given user can be detected with the aid of its T-domain group signature sequence as well as its F-domain spreading sequence, which can also be described as its user signature sequence. Since T-domain and F-domain detection are carried out separately, various detection algorithms can be invoked in the T-domain and F-domain detection stages. In this contribution, as examples, the decorrelating and the MMSE based MUD algorithms are investigated. The decorrelating MUD has the advantage of simplicity—each user can be detected independently, without requiring the knowledge of the received signal's amplitude, and without requiring the knowledge of the noise power. However, a disadvantage of the decorrelating MUD is that it amplifies the background noise. By contrast, the MMSE MUD is capable of suppressing the background noise with the aid of the knowledge of the SNRs associated with the users.

Let $Z_u[m]$ represent the receiver's output with respect to the mth subcarrier in the uth user group, after despreading using the uth group's T-domain signature sequence $a_u(t)$. Then, $Z_u[m]$ can be expressed as

$$Z_u[m] = \sqrt{\frac{P}{2M}} T_b \left\{ \sum_{\kappa=1}^{\mathcal{K}} b_{u\kappa} c_\kappa[m] + \sum_{\substack{n=1 \\ n \neq u}}^{N} \sum_{\kappa=1}^{\mathcal{K}} b_{n\kappa} c_\kappa[m] \rho_{un} + N_{um} \right\} \qquad u = 1, 2, \ldots, N; \quad m = 1, 2, \ldots, M \quad (23)$$

where N_{um} is a Gaussian random variable having zero-mean and a variance of $MN_0/2E_b$. Furthermore, the N number of outputs corresponding to the N number of user group signals and to the mth subcarrier can be written in a matrix form as

$$\mathbf{Z}[m] = \mathbf{R}_t \mathbf{b}_g + \mathbf{n}_m, \quad m = 1, 2, \ldots, M \quad (24)$$

where the common factor of $\sqrt{(P)/(2M)} T_b$ in (24) has been ignored for simplicity. In (24), the subscript g in $\mathbf{b}_g$ is used for emphasizing that the current detection stage is at the group level, while the subscript t associated with $\mathbf{R}_t$ emphasizes that it is the cross-correlation matrix of the T-domain spreading sequences. The rank of $\mathbf{R}_t$ is N. Furthermore, the terms in (24) are detailed as

$$\mathbf{Z}[m] = [Z_1[m], Z_2[m], \ldots, Z_N[m]]^T \quad (25)$$

$$\mathbf{b}_g = \left[\sum_{\kappa=1}^{\mathcal{K}} b_{1\kappa} c_\kappa[m], \sum_{\kappa=1}^{\mathcal{K}} b_{2\kappa} c_\kappa[m], \ldots, \sum_{\kappa=1}^{\mathcal{K}} b_{N\kappa} c_\kappa[m] \right]^T \quad (26)$$

$$\mathbf{n}_m = [N_{1m}, N_{2m}, \ldots, N_{Nm}]^T \quad (27)$$

$$\mathbf{R}_t = \begin{pmatrix} 1 & \rho_{12} & \cdots & \rho_{1N} \\ \rho_{21} & 1 & \cdots & \rho_{2N} \\ \vdots & \vdots & \ddots & \vdots \\ \rho_{N1} & \rho_{N2} & \cdots & 1 \end{pmatrix}. \quad (28)$$

Note that $\mathbf{n}_m$ of (27) is a zero-mean Gaussian random vector having a covariance matrix of

$$E\left[\mathbf{n}_m \mathbf{n}_m^T\right] = \frac{MN_0}{2E_b} \mathbf{R}_t. \quad (29)$$

With the aid of (24), we now characterize the separate MUDs invoked for detecting the TF-domain spread MC DS-CDMA signals.

1) Separate Decorrelating/MMSE Detector: In the context of the separate TF-domain decorrelating/MMSE MUD, the N variables of (24) associated with the N user groups are first processed by a decorrelator with respect to each of the M subcarriers. Specifically, the decorrelated group signals are obtained by multiplying both sides of

(24) with the inverse of the cross-correlation matrix $\mathbf{R}_t$ of the T-domain spreading sequences, which is expressed as

$$\mathbf{z}_m = \mathbf{R}_t^{-1}\mathbf{Z}[m] = \mathbf{b}_g + \mathbf{R}_t^{-1}\mathbf{n}_m, \quad m = 1, 2, \ldots, M \tag{30}$$

where $\mathbf{z}_m$ is a N-dimensional vector representing the soft outputs of the group-signal decorrelators corresponding to the N number of groups after the decorrelation process, and $\mathbf{R}_t^{-1}\mathbf{n}_m$ is a random Gaussian vector having the covariance matrix given by

$$E\left[\left(\mathbf{R}_t^{-1}\mathbf{n}_m\right)\left(\mathbf{R}_t^{-1}\mathbf{n}_m\right)^T\right] = \frac{MN_0}{2E_b}\mathbf{R}_t^{-1}. \tag{31}$$

After the decorrelation process, the composite multiuser signal contained in the nth user group is constituted by the nth element of $\mathbf{z}_m$, which is represented as $(\mathbf{z}_m)_n$ and can be expressed as

$$(\mathbf{z}_m)_n = \sum_{\kappa=1}^{\mathcal{K}} b_{n\kappa}c_\kappa[m] + (\mathbf{R}_t^{-1}\mathbf{n}_m)_n \quad n = 1, 2, \ldots, N; \quad m = 1, 2, \ldots, M. \tag{32}$$

With the aid of (32), the $\mathcal{K}$ number of users contained in the nth group can now be uniquely identified by their corresponding F-domain spreading sequences $\{\mathbf{c}_1, \mathbf{c}_2, \ldots, \mathbf{c}_\mathcal{K}\}$. The F-domain despread signal corresponding to the vth $(v = 1, 2, \ldots, \mathcal{K})$ user in the nth $(n = 1, 2, \ldots, N)$ group can be expressed as

$$\begin{aligned} F_{nv} &= \frac{1}{M}\sum_{m=1}^{M}(\mathbf{z}_m)_n \cdot c_v[m] \\ &= b_{nv} + \sum_{\substack{\kappa=1 \\ \kappa\neq v}}^{\mathcal{K}} b_{n\kappa}\beta_{v\kappa} + \frac{1}{M}\sum_{m=1}^{M}(\mathbf{R}_t^{-1}\mathbf{n}_m)_n c_v[m] \\ & \qquad n = 1, 2, \ldots, N; \quad v = 1, 2, \ldots, \mathcal{K} \end{aligned} \tag{33}$$

where β_{ij} is the correlation factor of the F-domain spreading sequences $\mathbf{c}_i$ and $\mathbf{c}_j$, as defined in Section III. Considering that there are $\mathcal{K}$ number of users in the nth group, the $\mathcal{K}$ number of variables expressed in the form of (33) can be written in a compact matrix form as

$$\mathbf{F}_n = \mathbf{R}_f\mathbf{b}_n + \mathbf{n}_f \tag{34}$$

where we have

$$\mathbf{F}_n = [F_{n1}, F_{n2}, \ldots, F_{n\mathcal{K}}]^T \tag{35}$$

$$\mathbf{b}_n = [b_{n1}, b_{n2}, \ldots, b_{n\mathcal{K}}]^T \tag{36}$$

$$\mathbf{R}_f = \begin{pmatrix} 1 & \beta_{12} & \ldots & \beta_{1\mathcal{K}} \\ \beta_{21} & 1 & \ldots & \beta_{2\mathcal{K}} \\ \vdots & \vdots & \ddots & \vdots \\ \beta_{\mathcal{K}1} & \beta_{\mathcal{K}2} & \ldots & 1 \end{pmatrix}. \tag{37}$$

In (34), the subscript f associated with $\mathbf{R}_f$ emphasizes that $\mathbf{R}_f$ is the cross-correlation matrix of the F-domain spreading sequences. Furthermore, in (34), $\mathbf{n}_f$ is a $\mathcal{K}$-dimensional random Gaussian vector having a zero-mean and a covariance matrix given by

$$E\left[\mathbf{n}_f\mathbf{n}_f^T\right] = \frac{N_0}{2E_b}\left(\mathbf{R}_t^{-1}\right)_{nn}\mathbf{R}_f. \tag{38}$$

Since the variance of the last term in (33) is $(N_0)/(2E_b)(\mathbf{R}_t^{-1})_{nn}$, which is independent of the index v, the MMSE solution based F-domain MUD can be implemented by multiplying both sides of (34) with $(\mathbf{R}_f + (N_0)/(2E_b)(\mathbf{R}_t^{-1})_{nn}\mathbf{I})^{-1}$, which is expressed as

$$\begin{aligned} &\left(\mathbf{R}_f + \frac{N_0}{2E_b}\left(\mathbf{R}_t^{-1}\right)_{nn}\mathbf{I}\right)^{-1}\mathbf{F}_n \\ &\quad = \left(\mathbf{R}_f + \frac{N_0}{2E_b}\left(\mathbf{R}_t^{-1}\right)_{nn}\mathbf{I}\right)^{-1}\mathbf{R}_f\mathbf{b}_n \\ &\qquad + \left(\mathbf{R}_f + \frac{N_0}{2E_b}\left(\mathbf{R}_t^{-1}\right)_{nn}\mathbf{I}\right)^{-1}\mathbf{n}_f \end{aligned} \tag{39}$$

while for each given user group n, where $n = 1, 2, \ldots, N$, the corresponding data bits $b_{n\kappa}$ are decided according to $\hat{b}_{n\kappa} = \text{sgn}(((\mathbf{R}_f + (N_0)/(2E_b)(\mathbf{R}_t^{-1})_{nn}\mathbf{I})^{-1}\mathbf{F}_n)_\kappa)$ for $\kappa = 1, 2, \ldots, \mathcal{K}$.

2) Separate MMSE/Decorrelating Detector: If we first process the N number of user group signals obeying (24) with the aid of the MMSE algorithm in the T-domain, then the MMSE based MUD's soft output can be expressed as

$$\begin{aligned} \mathbf{z}_m &= \left(\mathbf{R}_t + \frac{MN_0}{2E_b}\mathbf{I}\right)^{-1}\mathbf{Z}[m] \\ &= \left(\mathbf{R}_t + \frac{MN_0}{2E_b}\mathbf{I}\right)^{-1}\mathbf{R}_t\mathbf{b}_g + \left(\mathbf{R}_t + \frac{MN_0}{2E_b}\mathbf{I}\right)^{-1}\mathbf{n}_m \\ & \qquad m = 1, 2, \ldots, M. \end{aligned} \tag{40}$$

Let $(\mathbf{R}_t + (MN_0)/(2E_b)\mathbf{I})^{-1}\mathbf{R}_t = \{q_{ij}\}$. Then the nth element of $\mathbf{z}_m$ corresponding to the soft output matched to the nth group can be expressed as

$$(\mathbf{z}_m)_n = q_{nn}\sum_{\kappa=1}^{\mathcal{K}} b_{n\kappa}c_\kappa[m] + I_n + \left(\left(\mathbf{R}_t + \frac{MN_0}{2E_b}\mathbf{I}\right)^{-1}\mathbf{n}_m\right)_n \tag{41}$$

where $I_n = \sum_{\substack{i=1 \\ i\neq n}}^{N} q_{ni}\sum_{\kappa=1}^{\mathcal{K}} b_{i\kappa}c_\kappa[m]$ is the residual interference imposed by the other $(N-1)$ user groups after the MMSE processing.

Upon despreading $(\mathbf{z}_m)_n$ with the aid of the F-domain spreading sequences $\{\mathbf{c}_1, \mathbf{c}_2, \ldots, \mathbf{c}_\mathcal{K}\}$ employed by the $\mathcal{K}$ number of users in the nth group, it can be shown that the despread outputs can be expressed as

$$\mathbf{F}_n = q_{nn}\mathbf{R}_f\mathbf{b}_n + \mathbf{n}_f + \mathbf{I}_f \tag{42}$$

where $\mathbf{b}_n$ and $\mathbf{R}_f$ are given by (36) and (37), respectively, while

$$(\mathbf{n}_f)_\kappa = \frac{1}{M}\sum_{m=1}^{M}\left(\left(\mathbf{R}_t + \frac{MN_0}{2E_b}\mathbf{I}\right)^{-1}\mathbf{n}_m\right)_n \cdot c_\kappa[m] \quad \kappa = 1, 2, \ldots, \mathcal{K} \tag{43}$$

$$(\mathbf{I}_f)_\kappa = \frac{1}{M}\sum_{m=1}^{M} I_n \cdot c_\kappa[m], \quad \kappa = 1, 2, \ldots, \mathcal{K}. \tag{44}$$

Following the decorrelating-based processing of (42) using the inverse of $\mathbf{R}_f$, the decision variables associated with the $\mathcal{K}$ number of users in the nth group can be expressed as

$$\mathbf{R}_f^{-1}\mathbf{F}_n = q_{nn}\mathbf{b}_n + \mathbf{R}_f^{-1}\mathbf{n}_f + \mathbf{R}_f^{-1}\mathbf{I}_f \tag{45}$$

and the transmitted data bits of the users in the nth $(n = 1, 2, \ldots, N)$ group can be decided according to $\hat{b}_{n\kappa} = \text{sgn}((\mathbf{R}_f^{-1}\mathbf{F}_n)_\kappa)$ for $\kappa = 1, 2, \ldots, \mathcal{K}$.

V. Detection Complexity

We have investigated the detection of TF-domain spread MC DS-CDMA signals using the conventional decorrelating and/or MMSE multiuser detection algorithms. In the context of joint TF-domain MUDs, the joint TF-domain decorrelating detector and the joint TF-domain MMSE detector have been considered, which are characterized by (18) and (20), respectively. As shown in (18) and (20), the joint TF-domain decorrelating detector has to compute the inverse of $\mathbf{R}$, while the joint TF-domain MMSE detector has to determine the inverse of $(\mathbf{R} + (N_0)/(2E_b)\mathbf{I})$. The ranks of both of the preceding two matrices are determined by the number of users K, which may be as high as MN. Therefore, the complexity of the joint TF-domain decorrelating and MMSE detectors is on the order of $O(K^3)$ and $O(M^3N^3)$, respectively, when the system operates under full load. Furthermore, the joint TF-domain decorrelating and MMSE detectors designed for TF-domain spread MC DS-CDMA have the same detection complexity as the conventional decorrelating and MMSE detectors contrived for single-carrier DS-CDMA and the complexity of conventional MC-CDMA using F-domain spreading.

By contrast, in the context of separate TF-domain MUDs discussed in Section IV-B, the detectors are characterized by (30) and (39) when using the separate decorrelating/MMSE detector and by (40) and (45) when invoking the separate MMSE/decorrelating detector. The rank of the correlation matrices associated with the T-domain detection is N for both of these schemes, and the rank of the correlation matrices associated with the F-domain detection is $\mathcal{K}$, where $\mathcal{K}$ can be as high as M when the system is fully loaded. Hence, in the context of separate TF-domain detection, we have to compute the inverse of a N-rank matrix for the sake of T-domain detection associated with each of the M subcarriers, as well as the inverse of a $\mathcal{K}$-rank matrix associated with each of the N user groups for the sake of the corresponding F-domain detection. Notice that the inverse of the N-rank matrix required for T-domain detection only has to be computed once, and it can be used for all subcarriers. Similarly, the inverse of the $\mathcal{K}$-rank matrix required for F-domain detection is also computed only once, and it can be used for all user groups. Therefore, the complexity of the separate TF-domain detection schemes is on the order of $O(N^3 + \mathcal{K}^3)$, which is limited to $O(N^3 + M^3)$ when the system is fully loaded. For the separate TF-domain, detectors have to determine the inverses associated with each of the M subcarriers in the T-domain, and with each of the N user groups in the F-domain, the associated complexity is, hence, on the order of $O(MN^3 + N\mathcal{K}^3)$.

Based on the preceding discussions, we argue that separate TF-domain detectors have a lower detection complexity than joint TF-domain detectors. If the number of users is high, the benefit of decreasing the detection complexity is substantial. In the next section, we compare the BER performance of the detection schemes considered in the previous sections.

VI. Performance Results

In this section, we provide a range of simulation results in order to illustrate the achievable performance of TF-domain spread MC DS-CDMA in conjunction with the various detection schemes considered in Sections III and IV. As examples, we considered two TF-domain spread MC DS-CDMA schemes which use m-sequences [3] for both T-domain spreading and F-domain spreading. The first scheme used a T-domain spreading factor of $N = 15$ and an F-domain spreading factor of $M = 7$, while the second scheme used a T-domain spreading factor of $N = 7$ and an F-domain spreading factor of $M = 15$. Since, in both cases, we had $N \times M = 105$, the maximum number of users supported is 105. We considered three types of user loads: a light user load associated with $K = 45$ or 49 users, a moderate load associated with $K = 75$ or 77 users, and full load corresponding to $K = 105$ users.

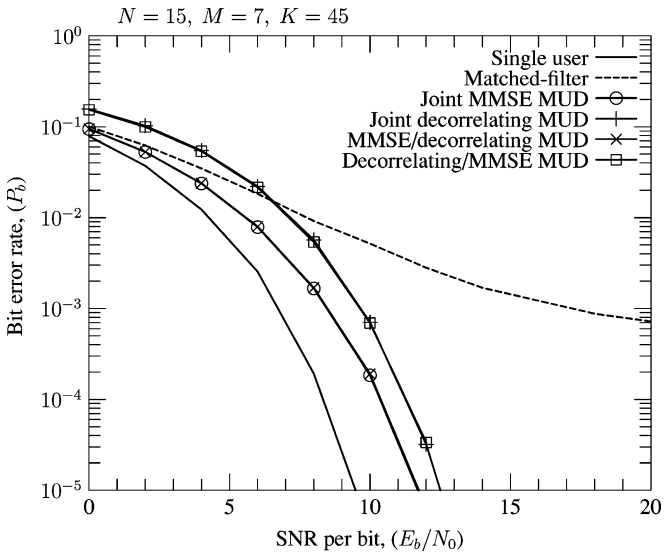

Fig. 3. BER performance comparison of the TF-domain spread MC DS-CDMA systems in conjunction with various detection schemes when using a T-domain spreading factor of $N = 15$, F-domain spreading factor of $M = 7$, and supporting a total of $K = 45$ users. The first of the detectors in the legends associated with separate TF-domain detection indicates the T-domain detection, and the second indicates the F-domain detection.

Fig. 3 compares the BER versus SNR per bit of E_b/N_0 performance of TF-domain spread MC DS-CDMA using the parameters of $N = 15, M = 7$ for the cases of load of $K = 45$. The results show that for all three types of load, the joint TF-domain MMSE MUD achieves the best BER performance, which is close to the single-user BER curve. By contrast, the correlation based detector exhibits the worst performance, in particular when E_b/N_0 is high. The BER curve of the correlation based detector exhibits an error floor at high SNR per bit value. The BER of the joint TF-domain decorrelating MUD is always higher than that of the joint TF-domain MMSE MUD, but as expected, it outperforms the correlation-based detector provided that the SNR per bit is sufficiently high. However, as seen in Fig. 3, the joint TF-domain decorrelating MUD may be outperformed by the correlation based detector if the SNR per bit value is very low. This is because it is widely recognized [19] that the decorrelating MUD amplifies the background noise while suppressing the multiuser interference. In the context of the separate TF-domain decorrelating/MMSE and the MMSE/decorrelating MUDs, we observe that both schemes outperform the joint TF-domain decorrelating MUD, while both both of them are outperformed by the joint TF-domain MMSE MUD. However, the BER performance of the separate TF-domain decorrelating/MMSE MUD is close to that of the joint TF-domain decorrelating MUD.

In Fig. 4, we compare the BER versus E_b/N_0 performance of TF-domain spread MC DS-CDMA using the parameters of $N = 7, M = 15$. The results show that all the arguments associated with Fig. 3 are applicable also in the context of these figures. As the results of Fig. 4 demonstrate, the joint TF-domain MMSE MUD outperforms the joint TF-domain decorrelating MUD, while the separate TF-domain decorrelating/MMSE and MMSE/decorrelating MUDs have a BER performance ranked between that achieved by the TF-domain MMSE MUD and that achieved by the joint TF-domain decorrelating MUD. Furthermore, for the cases of light and moderate load, the BER

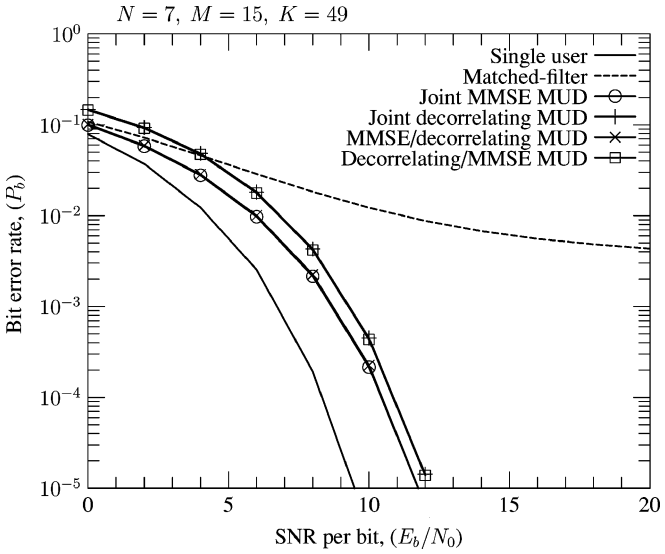

Fig. 4. BER performance comparison of the TF-domain spread MC DS-CDMA systems associated with various detection schemes when using a T-domain spreading factor of $N = 7$, F-domain spreading factor of $M = 15$, and supporting a total of $K = 49$ users.

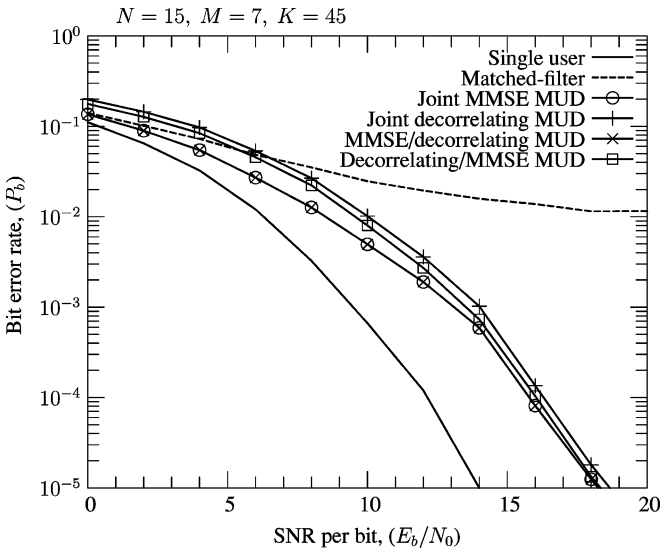

Fig. 5. BER performance comparison of the TF-domain spread MC DS-CDMA systems in conjunction with various detection schemes when using a T-domain spreading factor of $N = 15$, F-domain spreading factor of $M = 7$, and supporting a total of $K = 45$ users, where each subcarrier is experienced with uncorrelated flat Rayleigh fading.

performance of the separate TF-domain decorrelating/MMSE MUD is close to that of the joint TF-domain decorrelating MUD. By contrast, the BER performance of the separate TF-domain MMSE/decorrelating MUD is close to that of the joint TF-domain MMSE MUD.

Finally, Figs. 5 and 6 illustrate the BER performance of the TF-domain spreading assisted MC DS-CDMA system in conjunction with different MUDs and a matched filter, when communicating over an uncorrelated Rayleigh fading channel. Comparing these figures to Figs. 3 and 4, we may conclude that all these MUD techniques exhibit similar performance trends in a Rayleigh fading channel to those experienced over AWGN channels.

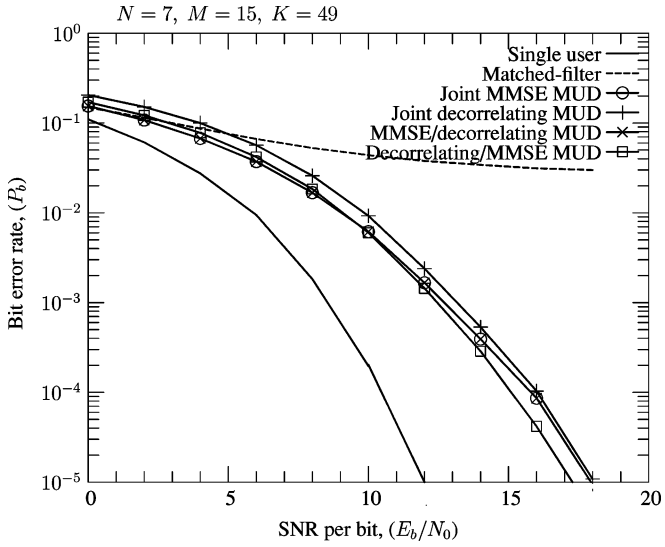

Fig. 6. BER performance comparison of the TF-domain spread MC DS-CDMA systems in conjunction with various detection schemes when using a T-domain spreading factor of $N = 7$, F-domain spreading factor of $M = 15$, and supporting a total of $K = 49$ users, where each subcarrier is experienced with uncorrelated flat Rayleigh fading.

VII. Conclusion

In summary, in this contribution, we have proposed and studied a MC DS-CDMA scheme which employs both T-domain and F-domain spreading. We have investigated both joint and separate TF-domain detection of the TF-domain spread MC DS-CDMA signals. In order to characterize the performance and the advantages of the proposed TF-domain spread MC DS-CDMA scheme, we have investigated and compared its BER performance in conjunction with a range of detectors. These detectors include the single-user correlation based detector, the joint TF-domain decorrelating MUD, the joint TF-domain MMSE MUD, the separate TF-domain decorrelating/MMSE MUD, and the separate TF-domain MMSE/decorrelating MUD. The results of our study demonstrate that the separate TF-domain MUD schemes are capable of achieving a similar BER performance to that of the joint TF-domain MUD schemes, while imposing a significantly lower detection complexity than the joint TF-domain MUD schemes. Due to its low detection complexity, the employment of TF-domain spread MC DS-CDMA invoking separate TF-domain MUDs is beneficial in the context of broadband wireless systems supporting a large number of users.

References

[1] M. B. Pursley, "Performance evaluation for phase-coded spread-spectrum multiple-access communication-Part I: System analysis," *IEEE Trans. Commun.*, vol. COM-25, no. 8, pp. 795–799, Aug. 1977.

[2] M. K. Simon, J. K. Omura, R. A. Scholtz, and B. K. Levitt, *Spread Spectrum Communications: Volume I*. Rockville, MD: Computer Science, 1985.

[3] R. E. Ziemer and R. L. Peterson, *Digital Communications and Spread Spectrum Systems*. New York: Macmillan, 1985.

[4] A. Chouly, A. Brajal, and S. Jourdan, "Orthogonal multicarrier techniques applied to direct sequence spread spectrum CDMA systems," *Proc. IEEE GLOBECOM'93*, pp. 1723–1728, Houston, TX, Nov. 1993.

[5] L. Hanzo, L.-L. Yang, E.-L. Kuan, and K. Yen, *Single- and Multi-Carrier DS-CDMA: Multi-User Detection, Space-Time Spreading, Synchronisation, Standards and Networking*. Piscataway, NJ: IEEE Press, Wiley, 2003, p. 1060.

[6] N. Yee, J.-P. Linnartz, and G. P. Fettweis, "Multicarrier CDMA in indoor wireless radio networks," *Proc. PIMRC'93*, pp. 109–113, 1993.

[7] K. Fazel and L. Papke, "On the performance of convolutionally-coded CDMA/OFDM for mobile communication systems," in *Proc. PIMRC'93*, 1993, pp. 468–472.
[8] X. Gui and T. S. Ng, "Performance of asynchronous orthogonal multicarrier CDMA system in frequency selective fading channel," *IEEE Trans. Commun.*, vol. 47, no. 7, pp. 1084–1091, Jul. 1999.
[9] R. Prasad and S. Hara, "Overview of multicarrier CDMA," *IEEE Commun. Mag.*, vol. 35, no. 12, pp. 126–133, Dec. 1997.
[10] E. S. Sousa, "Performance of a direct sequence spread spectrum multiple access system utilizing unequal carrier frequencies," *IEICE Trans. Commun.*, vol. E76-B, pp. 906–912, Aug. 1993.
[11] L. Vandendorpe, "Multitone direct sequence CDMA system in an indoor wireless environment," in *Proc. IEEE 1st Symp. Communications and Vehicular Technology, Benelux, Delft, The Netherlands*, Oct. 1993, p. 4.1-–4.1-8.
[12] E. A. Sourour and M. Nakagawa, "Performance of orthogonal multicarrier CDMA in a multipath fading channel," *IEEE Trans. Commun.*, vol. 44, no. 3, pp. 356–367, Mar. 1996.
[13] S. Kondo and L. B. Milstein, "Performance of multicarrier DS CDMA systems," *IEEE Trans. Commun.*, vol. 44, no. 2, pp. 238–246, Feb. 1996.
[14] L.-L. Yang and L. Hanzo, "Blind joint soft-detection assisted slow frequency-hopping multicarrier DS-CDMA," *IEEE Trans. Commun.*, vol. 48, no. 9, pp. 1520–1529, Sep. 2000.
[15] L.-L. Yang and L. Hanzo, "Slow frequency-hopping multicarrier DS-CDMA for transmission over Nakagami multipath fading channels," *IEEE J. Sel. Areas Commun.*, vol. 19, no. 7, pp. 1211–1221, Jul. 2001.
[16] L.-L. Yang and L. Hanzo, "Performance of generalized multicarrier DS-CDMA over Nakagami-m fading channels," *IEEE Trans. Commun.*, vol. 50, no. 6, pp. 956–966, Jun. 2002.
[17] C. W. You and D. S. Hong, "Multicarrier CDMA systems using time-domain and frequency-domain spreading codes," *IEEE Trans. Commun.*, vol. 51, no. 1, pp. 17–21, Jan. 2003.
[18] M. Progler, C. Evci, and M. Umehira, "Air interface access schemes for broadband mobile systems," *IEEE Commun. Mag.*, vol. 37, no. 9, pp. 106–115, Sep. 1999.
[19] S. Verdu, *Multiuser Detection*. Cambridge, U.K.: Cambridge Univ. Press, 1998.
[20] A. J. Viterbi, *CDMA: Principles of Spread Spectrum Communications*. Reading, MA: Addison-Wesley, 1995.
[21] V. M. Dasilva and E. S. Sousa, "Multicarrier orthogonal CDMA signals for quasi-synchronous communication systems," *IEEE J. Sel. Areas Commun.*, vol. 12, no. 5, pp. 842–852, Jun. 1994.
[22] H. V. Poor and S. Verdu, "Probability of error in MMSE multiuser detection," *IEEE Trans. Inf. Theory*, vol. 43, no. 3, pp. 858–871, May 1997.

Improved Channel Decoding for the CDMA Forward Link Chip-Level LMMSE Receiver

Geoffrey G. Messier and Witold A. Krzymień

***Abstract*—This paper investigates how to improve channel decoder trellis path metric calculations when convolutional or turbo codes are combined with the chip-level linear minimum mean square error (LMMSE) code division multiple access (CDMA) mobile receiver. These metric calculations require channel state information (CSI) that consists of desired signal amplitude and interference plus noise variance. Several techniques suitable for use with the chip-level LMMSE receiver are presented for estimating CSI. Chip-level simulations are used to evaluate CDMA forward link performance when these techniques are used by the mobile. The results indicate that the channel state estimation scheme that provides the best forward link performance depends on the type of channel code and channel decoder algorithm used in the system.**

***Index Terms*—Channel state estimation, code division multiple access (CDMA), LMMSE equalization, Rake receiver, turbo codes.**

I. Introduction

The work presented in this paper aims to improve the performance of both convolutional and turbo codes on the code division multiple access (CDMA) forward link when the chip-level linear minimum mean square error (LMMSE) receiver is used in the mobile. This improvement is achieved by using estimation techniques that provide the mobile channel decoder with better channel state information (CSI). The chip-level LMMSE receiver has received considerable attention in the area of CDMA forward link advanced receiver research [1]–[3]. It cancels CDMA forward link intracell interference by equalizing the received chip waveform and restoring the orthogonality of the forward link Walsh spreading sequences.

The performance of turbo codes with chip-level LMMSE equalization and LogMAP decoding has been investigated by Hooli *et al*. [4]. In that paper, pilot symbols embedded in the traffic transmission are used to estimate CSI. However, Hooli *et al*. do not consider the variety of other CSI estimation schemes that could be used with the chip-level LMMSE receiver or investigate how these schemes could affect forward link performance. They also do not consider turbo decoding with the soft-output Viterbi decoder (SOVA) algorithm, which, as this paper will illustrate, has very different channel state estimation requirements than the LogMAP decoder.

Several alternatives have been proposed for channel state estimation when the mobile uses the conventional RAKE receiver. Worm *et al*. advocate using the SOVA turbo decoder metric without any CSI [5]. Summers and Wilson [6] present an "online" SNR estimation technique for turbo decoding in a time-invariant AWGN channel that has been extended by Ramesh *et al*. to wireless applications [7], [8]. The authors have also developed channel state estimation techniques for the CDMA forward link that improve convolutional and turbo code performance for mobiles with conventional RAKE receivers [9], [10].

Manuscript received August 20, 2003; revised April 15, 2004, November 22, 2004 and March 23, 2005. This work was supported by TRlabs, the Natural Sciences and Engineering Research Council (NSERC) of Canada, and the Alberta Informatics Circle of Research Excellence (iCORE). The review of this paper was coordinated by Prof. M. Juntti.

G. G. Messier is with the Department of Electrical and Computer Engineering, University of Calgary and TRLabs, Calgary, AB T2N 1N4, Canada (e-mail: gmessier@ucalgary.ca).

W. A. Krzymień is with the Department of Electrical and Computer Engineering, University of Alberta and TRLabs, Edmonton, AB T6G 2V4, Canada (e-mail: wak@ece.ualberta.ca).

Digital Object Identifier 10.1109/TVT.2005.861168